ELSEVIER

Ceramics International 30 (2004) 257–265

CERAMICS INTERNATIONAL

www.elsevier.com/locate/ceramint

Effects of processing parameters on the fabrication of near-net-shape fibre reinforced oxide ceramic matrix composites via sol–gel route

M.K. Naskar[a], M. Chatterjee[a,*], A. Dey[a], K. Basu[b]

[a]*Sol–Gel Division, Central Glass & Ceramic Research Institute, Kolkata 700 032, India*
[b]*Regional Research Laboratory, Bhopal 462 026, India*

Received 5 March 2003; received in revised form 12 March 2003; accepted 2 May 2003

Abstract

The sol infiltration technique was found to be very effective for the fabrication of near-net-shape mullite fibre reinforced ceramic matrix composites (CMCs). The infiltrated sol, in single- and bi-component oxide systems with equivalent molar compositions of Al_2O_3 (A), 60 Al_2O_3:40 SiO_2 (AS), 87 Al_2O_3: 13 ZrO_2 (AZ), and 94 ZrO_2:06 Y_2O_3 (ZY), after drying and calcination, formed the matrix. The discontinuous mullite fibres (as preforms with 15 vol.% fibre content) acted as the reinforcement agents. The characteristics of the CMCs were found to be strongly dependent on the type of the sols (infiltrates) and their viscosity, presence of non-reactive fillers in the sol, number of infiltrations, intermediate and final sintering temperatures and in-situ deposition of carbon in the fabricated materials. The CMCs were characterised by X-ray diffraction (XRD), scanning electron microscopy (SEM) and the three point bend test. SEM indicated fibre pull-out in the fracture surface of the CMCs. The pseudo-ductile character, developed in the CMCs, was evident from the load–elongation curve of the three-point bend test. The carbon-containing CMCs exhibited a modulus value of almost 51 GPa.

Keywords: A: Sol–gel process; B: Composites; C: Mechanical properties; D: Mullite; E: Structural applications

1. Introduction

Ceramic fibre reinforced ceramic matrix composites (CMCs) are considered as promising candidates for use in high temperature structural application due to their high strength, high modulus and toughness. The fibre reinforced ceramic materials have been successful in eliminating the catastrophic behaviour of monolithic ceramics [1,2]. Incorporation of reinforcing inorganic fibres into the ceramic matrix develops CMCs which exhibit pseudo ductility, preventing catastrophic crack growth by such mechanisms as crack bridging, fibre debonding, fibre pull-out [1–7]. The characteristics of the CMCs will depend upon the shape, size and dispersion of the reinforcement, the microstructure of the ceramic matrix and the physicochemical nature of the interface between the fibres and the matrix. The interaction between the fibre and the matrix is expected to take place and judicious control of processing parameters is necessary to establish the optimum degree of interfacial bonding [1,7].

Although numerous processing methods are already known for producing CMCs, e.g. polymer impregnation and pyrolysis, melt infiltration, chemical vapour infiltration (CVI), hot pressing and sol–gel [4,5,8,9], the sol–gel infiltration has proved to be a viable technique for fabrication of CMCs using fibrous preforms as the precursor materials, as the method involves several advantages, such as better homogeneity, low processing temperatures, near-net-shape fabrication [9]. However, the technique requires multiple infiltration with intermediate heat-treatment to overcome matrix cracking due to excessive shrinkage of matrix during drying and sintering [1,4,8,9], Further, well dispersed fillers, i.e.

* Corresponding author. Tel.: +91-33-2483-8086; fax: +91-33-2473-0957.
E-mail address: minati33@hotmail.com (M. Chatterjee).

0272-8842/03/$30.00
doi:10.1016/S0272-8842(03)00097-X

Table 1
Characteristics of the parent sols (infiltrates)

Sol designation	Composition (mol%)	pH	Viscosity (mPa s)
ZY	ZrO2:Y_2O_3 = 94:06	2.53±0.01	3±1
A	Al_2O_3 = 100	4.91±0.01	4±1
AS	Al_2O_3:SiO_2 = 60:40	3.96±0.01	6±1
AZ	Al_2O_3:ZrO_2 = 87:13	3.21±0.01	10±1

submicron particles in the sol may also counter matrix shrinkage [8,10–12], thereby enhancing characteristics of CMCs. Keeping the afore-mentioned points in view, an attempt has been made in the present investigation: (i) to examine the effects of processing parameters on the fabrication of near-net-shape CMCs using discontinuous mullite fibre preforms (15 vol.% fibre content) as the reinforcement agent and single- and bi-component oxides in systems with molar compositions Al_2O_3, 60 Al_2O_3:40 SiO_2, 87 Al_2O_3:13 ZrO_2 and 94 ZrO_2:06 Y_2O_3 as the matrix materials, based on the vacuum sol infiltration technique, (ii) to characterize the developed CMCs by different analytical techniques and (iii) to examine the characteristics of the fibre/matrix interface by in-situ deposition of carbon in the matrix material.

2. Experimental procedure

2.1. Preparation of precursor fibre preforms

Samples of dimensions 40 mm×7 mm×6 mm were cut from as-received 15% volume fraction discontinuous mullite fibre preforms of 100 mm diameter and 10mm thickness (from M/s Orient Cerlane Limited, Gujrat) for investigating and establishing the parameters of sol infiltration technique for the fabrication of near-net-shape CMCs. The samples were activated at 200 °C (at the heating rate of 1 °C/min) with a dwell time of 1 h to remove most of volatiles, if any, absorbed on the fibre surface and the intra-fibre regions of the sample preform. The activated precursor fibre preform samples were preserved in a desiccator maintained at a relative humidity of 25%. These samples will function as the reinforcing material.

2.2. Preparation of single- and bi-component infiltrates (liquid matrix precursor) for the fabrication of CMCs

2.2.1. Preparation of alumina (single-component) sol

For the preparation of a parent aqueous alumina sol, $Al(NO_3)_3.9H_2O$ (Guaranteed Reagent (G.R.), Merck, India with purity >99% was used as the starting material [13]. Boelunite particles were precipitated from this aluminium nitrate solution at 80–90 °C, with ammonia solution (25 wt.% G.R., Merck, India). The washed precipitate was peptized with nitric acid (69 wt.%, G.R. Merck, India) to obtain a colloidal sol. The pH and viscosity of the present sol (designated as 'A') were 4.91±0.01 and 4±1 mPa s respectively (Table 1). From this parent sol, several sols of different viscosities were prepared by solvent evaporation (Table 2). The pH of the sols was measured with a Jencon pH meter (model: 3030) while the viscosity values were recorded using a Brookfield viscometer (model: LVTDV-II).

2.2.2. Preparation of alumina-silica (bi-component) sol

A calculated quantity of tetraethylorthosilicate, TEOS, (purity 98%; Fluka Chemie AG, Switzerland) was slowly added to the parent alumina sol prepared as in Section 2.2.1 under stirring. The molar ratio of alumina to silica in the bi-component colloidal sol was

Table 2
Characteristics of some typical CMCs obtained under different experimental conditions

Sample no.	Sol viscosity (mPa s)	No. of infiltration	Intermediate sintering temperature (°C)	Final sintering temperature (°C)	Flexural strength (MPa)	Characteristics of the products
ZY1	60±1(1)+40±1(2)	3	800	1400	5.2	Good surface (pseudo ductility)
ZY2	60±1(1)+40±1(4)	5	800	1200	7.3	Brittle, good surface (ceramic character)
ZY3	60±1(1)+40±1(4)	5	800	1400	13.9	Brittle, good surface (ceramic character)
ZY4	40±1 (5)	5	800	1400	6.8	Good surface (pseudo ductility)
ZY5	60±1(1)+40±1(2)	3	500	1000[a]	6.3	Good surface (pseudo ductility)
ZY6	60±1(1)+40±1(2)	3	500	1400[a]	6.2	Good surface (pseudo ductility)
A1	40±1(1)+20±1(4)	5	400	1400	2.8	Brittle, good surface (ceramic character)
A2	30±1(5)	5	400	1400	2.4	Good surface (pseudo ductility)
AS1	60±1(1)+14±1(4)	5	400	1400	4.8	Brittle, good surface (ceramic character)
AS2	40±1(1)+14±1(4)	5	400	1400	4.2	Good surface (pseudo ductility)
AZ1	60±1(3)+40±1(1)	4	400	1400	3.0	Good surface (pseudo ductility)
AZ2	60±1(3)+40±1(2)	5	400	1400	3.8	Brittle, good surface (ceramic character)

Figures in parentheses indicate the number of infiltration.
[a] N_2 atmosphere.

maintained at 60:40 (mullite composition). The pH and viscosity of the parent bicomponent sol (designated as 'AS') was 3.96±0.01 and 6±1 mPa s respectively (Table 1). From this parent sol, several sols of different viscosities were prepared by solvent evaporation (Table 2) as described in Section 2.2.1.

2.2.3. Preparation of alumina–zirconia (bi-component) sol

The precursor materials for the preparation of alumina–zirconia sols with the Al_2O_3:ZrO_2 molar ratios of 87:13 were aluminium nitrate nonahydrate, $Al(NO_3)_3.9H_2O$ (G.R, Merck, India, purity >99%) and zirconium oxychioride octahydrate, $ZrOCl_2.8H_2O$, (Indian Rare Earths Limited, purity >99%). An aqueous solution with Al^{3+} concentration of 1.5 M was prepared by dissolving the aluminium nitrate in deionised water (conductivity of deionised water: $\sim 1.4\times10^{-5}$ mho). The calculated quantity of zirconium oxychlonde solution with Zr^{4+} concentration of 1.5 M in deionised water was added to the aluminium nitrate solution. The resulting solution was then subjected to sol formation at 80°±1 °C by the addition of concentrated ammonia solution (25 wt.%, G.R., Merck, India). The final viscosity of the transparent bi-component sols (designated as AZ) was determined to be 10±1 mPa s. The pH of the sol at this stage was found to be 3.21±0.01 (Table 1). From the bi-component sol, i.e. $87Al_2O_3.13ZrO_2$ in equivalent oxide mole content, several sols of viscosities ranging from 40 to 60 mPa s were prepared by solvent evaporation (Table 2).

2.2.4. Preparation of zirconia–ytiria (bi-component) sol

For the preparation of zirconia (ZrO_2) sols, stabilised with 6 mol% Y_2O_3, zirconium oxychionde octahydrate ($ZrOCl_2.8H_2O$) and hydrous yttrium nitrate (both from M/s Indian Rare Earths Limited, Mumbai), each with a purity of about 99.9%, were used as the starting materials [14,15]. Precipitates of hydrated zirconia were obtained by adding aqueous ammonia solution (25 wt.%, G.R., Merck, India) to a solution of zirconium oxychloride octahydrate in deionized water. The washed precipitate was peptised with glacial acetic acid (99.8%, AnalaR, BDH, India) at 65°±1°C. The sol thus obtained had a Zr^{4+} concentration of 1.2M.

To a known volume of the zirconium acetate sol, a required amount of yttrium nitrate (6 mol% equivalent Y_2O_3) was mixed under stirring. The pH and viscosity of the resulting yttrium containing zirconia sol (parent sol), designated as ZY, was found to be 2.53±0.01 and 3±1 mPa s respectively (Table 1). No organics were added to the sol as viscosity controlling agent. From the parent sol, several sols of viscosities ranging from 40±1 to 60±1 mPa s (Table 2) were prepared by solvent evaporation. Table 1 summarises the characteristics of sols used in the present investigation.

2.2.5. Preparation of stabilised zirconia (with the molar composition ZrO_2:Y_2O_3 as 94:6) powder (filler)

A known amount of the parent ZY sol (Section 2.2.4) was evaporated to dryness at about 80 °C and the resulting gel powder was subjected to calcination at 800 °C with 1 h dwell time in air under static condition followed by grinding. The calcined powder was used as the filler and dispersed in the ZY sol which was subsequently used as the infiltrate for the fabrication of CMCs.

2.3. Preparation of CMCs by vacuum infiltration technique (VIT)

In the present investigation, the vacuum infiltration technique [9,16] using four different sols of various viscosities (Tables 1 and 2) as the infiltrates was followed. To carry out the infiltration experiments, a laboratory made set-up was used. Activated, precursor preforms of dimensions 40 mm×7 mm×6 mm were immersed in the sol for 10 min on the bed of a specially designed infiltration unit. The sol was then removed slowly (3–5 ml/min) by a rotary vacuum pump (model: TSRP/100) attached to the infiltration unit. The infiltrated preform samples were placed in air at ambient temperature for converting the sol penetrated into the preform to the corresponding gel. The samples were further dried in an air circulating oven at 100±2 °C for 4 h and subsequently calcined (intermediate heating) at 400, 500 and 800 °C (according to the necessity) in air under static condition to remove the volatiles and decomposable materials. Calcining lead to the formation of voids and cracking of matrix due to shrinkage. The above infiltration process was repeated to examine the effect of number of infiltrations on the characteristics of the CMCs. Final sintering of the infiltrated preforms were performed at 1000, 1200 and 1400 °C in air under static condition. All the CMCs were white in colour. For the preparation of carbon containing CMCs, the intermediate heating of the infiltrated ZY containing preforms were performed at 500 °C with a dwell time of 1 h in static air followed by the final calcination at 1000 and 1400 °C, each for 1 h in nitrogen (N_2) atmosphere with a flow rate of N_2 as 1 l/min (Sample nos. ZY5 and ZY6 of Table 2). The CMCs obtained in N_2 atmosphere were black in colour.

2.4. Characterisation of the materials

(a) The as-received fibres of tensile strength of about 2.5 GPa and modulus of about 100 GPa were characterised by: (1) XRD: (model: Philips PW 1730) using Ni-filtered CuK_α radiation (ii) (SEM: model: Leo 400c) on samples of dimensions 2 mm×2 mm×1 mm and (iii) wet chemical analysis.

(b) The infiltrated materials (CMCs) were characterised by (i) XRD as described previously in Section 2.4 (a), (ii) SEM in which the fracture surfaces and the top surfaces of samples of the CMCs of same dimensions were examined as mentioned in Section 2.4 (a), (iii) thermogravimetry analysis (TGA) (Model: Netzsch STA 409c) from 30 to 1000 °C with a heating rate of 10 °C/mm in argon atmosphere and (iv) the flexural strength and modulus measurement on samples of dimensions 40 mm×7 mm×6 mm using three point bend test (Instron Universal Testing Machine, model: 5500 R) under a cross-head speed of 0.5 mm/min. Each strength datum is an average over six samples.

(c) The stabilised zirconia powder (with the molar composition of ZrO_2:Y_2O_3 as 94:06) was characterised by: (i) XRD and (ii) SEM as described earlier and (iii) particle size analyser (Model: Autosizer IIC, Malvern Instruments).

3. Results and discussion

3.1. Characteristics of the precursor preforms

The XRD of the precursor preforms used in the present investigation indicated the presence of mullite as the only phase. The microstructural feature of the preform in Fig. 1 indicates that the fibres are circular in diameter with the diameter distribution in the range 3–8 μm. The shot-content in the fibre preform was found to be negligible. Presence of considerable amounts of inter-fibre pores and voids is evident from the microstructure. Infiltration of the sol in the preform is expected to fill these inter-fibre pores and voids, leading to the formation of the continuous phase, i.e. the matrix, which is the primary aim of this investigation. The preforms were found to contain 54.88 wt.% SiO_2 and 43.05 wt.% Al_2O_3 as the major constituents with trace impurities of Fe_2O_3, TiO_2, K_2O, Na_2O and LOI.

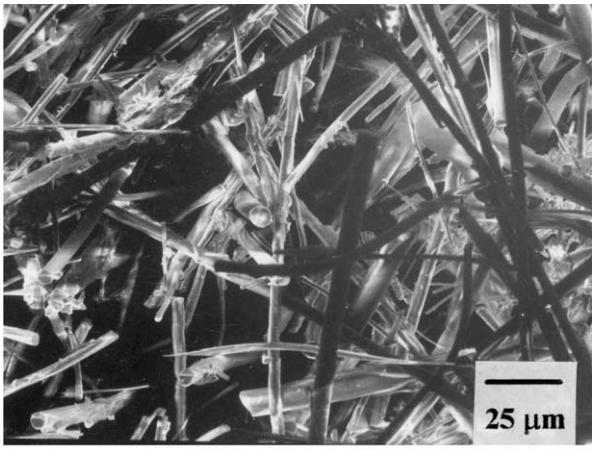

Fig. 1. SEM of the preform showing inter-fibre voids and porosities.

3.2. Characteristics of the infiltrates (sols)

Table 2 summarises the characteristics of CMCs fabricated using sols of different viscosities in single- and bi-component oxide systems following VIT. In the present investigation, four different types of sols (Table 1) were considered. It is to be noted that for each type of the sol, the higher the viscosity, the more difficult it was to achieve good wetting of the fibres by the sol and infiltrate the sol into the interconnected pores and voids [9,10,16]. Further, infiltration of the high viscosity sols gave rise to the formation of considerable amounts of air bubbles during operation and deposition of fragmented coatings on the surface of the preform after drying which prevented further penetration of sols inside the preform during repeated infiltration. On the other hand, sols of low viscosity were also found to be unsuitable because in such cases even after nine cycles of infiltration, the sample exhibited considerably brittle character. Based on the above results, in the present investigation, the viscosity of each type of sol was kept fixed in certain optimum ranges (Table 2) which in turn were found to depend on their polymerisation behaviour and preparative principles. pH of the sol is also an important point to be considered, as it affects both the viscosity and stability of a sol. With the increase in pH, viscosity of a sol increased and finally caused gel formation. Thus, an optimum value of both the pH and viscosity of different sols are necessary for carrying out the infiltration experiments [1].

3.3. Characteristics of the CMCs obtained by the sol infiltration technique

Characteristics of the CMCs fabricated under different experimental conditions have been presented in Table 2. As described in Table 2, characteristics of the CMCs have been found to be affected by the following factors.

3.3.1. Cracking in the matrix of the CMCs

Although the sol infiltration technique of fabricating CMCs has several advantages, such as, homogeneous mixing of the multicomponent oxides, higher purity, low processing temperature, the method suffers from the serious problem of excessive shrinkage during drying due to removal of considerable amount of volatiles, giving rise to extensive matrix cracking and residual fine scale porosity in composites followed by degradation of mechanical properties. In the present investigation, this problem was tried to be minimised by (i) multiple infiltration of the infiltrated preform followed by intermediate heat-treatment at the lowest possible temperature for

avoiding fibre/matrix reaction [1,8,9] and (ii) adding non-reactive fillers to the sol to counter this shrinkage [10–12]. Multiple infiltration in the green state helps to improve the green strength and green machinability and handling. Table 2 indicates that initial infiltration with a sol of high viscosity, followed by intermediate sintering and further infiltration with a sol of low viscosity, minimises matrix cracking and improves the flexural strength of the CMCs (Sample nos. ZY1 and AS2 of Table 2). Fig. 2 represents the SEM of the fracture surface of the Sample no. ZY1 of Table 2 after three-point bend test which indicates fibre pull-out in the sample while the load–elongation curve in Fig. 3 reflects the development of pseudoductile character in the same sample. In contrast to Sample no. ZY1, the Sample no. ZY3 of Table 2 fails to exhibit pseudo ductility. Development of strong interaction at the fibre/matrix interface may be the reason of such failure. This is reflected from the load-elongation curve of the three point bend test presented in Fig. 4. Fig. 5 represents the SEM of the fracture surface after three point bend test of the Sample no. ZY3 of Table 2. Filling up inter-fibre voids and pores by infiltration of excess sol through increasing number of infiltrations dramatically changed the fibre/matrix characteristics, leading to the formation of ceramic materials with monolithic character. Therefore an optimum number of infiltration is necessary for obtaining CMC with desired mechanical properties.

It has been reported [10–12] that the addition of non-reactive solid particles (fillers) to the sol increases infiltration efficiency and reduces matrix cracking by minimizing shrinkage. Comparing the results of Sample nos. ZY1 and ZY4 of Table 2, it is observed that the addition of 10 wt.% of sol–gel derived ZY powder (Section 2.2.5), with the tetragonal (t-) and cubic (c-) ZrO_2 and mean size of about 0.5 μm to the ZY sol (as the infiltrate) helped to modify the fibre/matrix interface characteristics of the developed CMCs. The dispersed particles in the sol produced unaggregated colloidal particles. Both the particle size and loading of the fillers in the sol are the dominant factors for controlling the characteristics of the CMCs, thereby tailoring the fibre/matrix interaction. As the addition of fillers caused an increase in the viscosity of the sol [1], a maximum loading up to about 10 wt.% was found to be the optimum in the present case. Figs. 6 and 7 represent the particle

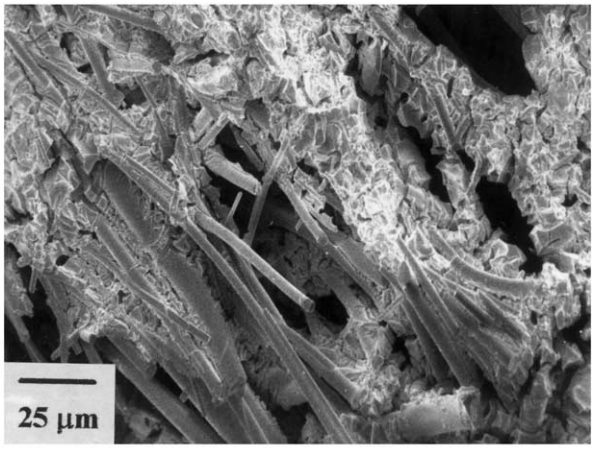

Fig. 2. SEM of the fracture of CMC after three-point bend test (Sample no. ZY1 of Table 2) showing fibre pull-out from the matrix.

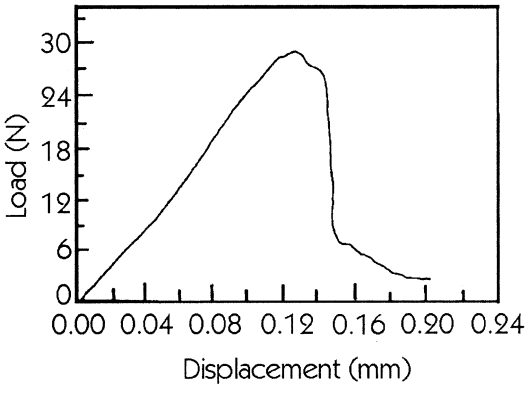

Fig. 3. Load–displacement curve of sample no. ZY1 of Table 2.

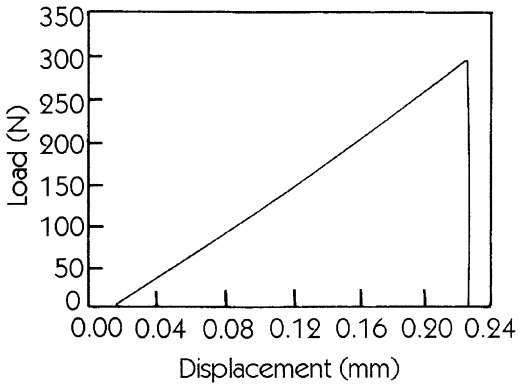

Fig. 4. Load–displacement curve of sample no. ZY3 of Table 2.

Fig. 5. SEM of the fracture surface of CMC after three-point bend test (sample no. ZY3 of Table 2).

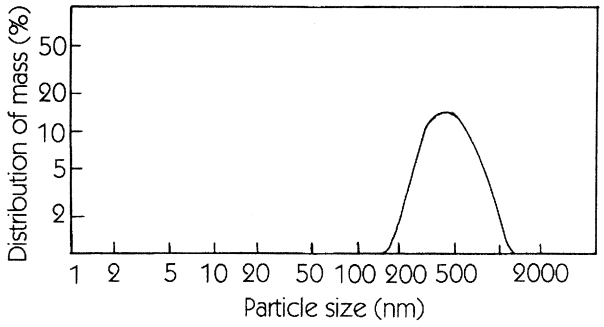

Fig. 6. Particle size distribution of the sol-gel derived ZY particles (fillers).

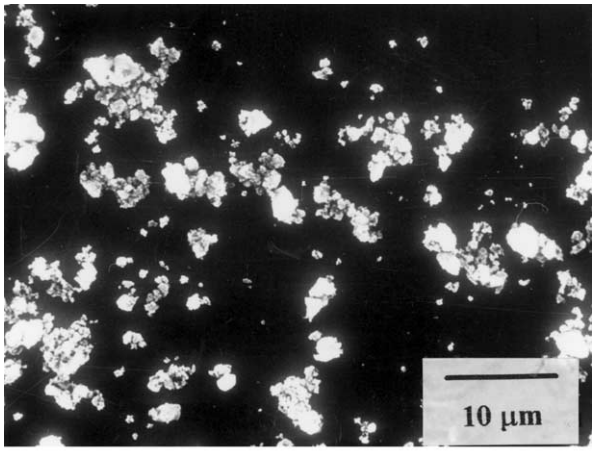

Fig. 7. SEM of the sol-gel derived ZY particles (fillers) showing the formation of submicrometre sized particles.

size distribution and SEM, respectively of the ZY particles used as fillers in the present study. Both the figures indicate the formation of submicrometre sized particles. It is to be noted that although attempts were made to increase the flexural strength of CMCs by optimising different process parameters, however, insignificant improvements in the results were obtained in these preliminary experiments. Further work in this area to improve the strength values is under study.

3.3.2. Intermediate and final sintering temperature

It has already been mentioned in Section 3.3.1 that the multiple infiltration followed by intermediate sintering minimise matrix cracking, thereby enhancing the mechanical properties. Unless the decomposable materials present in the green body, after each infiltration, are properly removed during intermediate sintering steps, high strength of the CMCs is difficult to attain. The choice of this intermediate sintering temperature, however, depends on the system under consideration. Fourier transform infrared (FTIR) spectra of the sol–gel CaO-doped ZrO_2 fibres prepared from the zirconium acetate sols and calcined at different temperatures from 30 to 1000 °C had confirmed the removal of almost all the decomposable and carbonaceous materials at 800 °C [17] with the formation of white coloured fibres. Based on this result, the intermediate sintering temperature of 800 °C was selected for multiple infiltration of ZY sol for fabrication of CMCs in the present investigation. For the other sols, i.e. A, AZ and AS, based on their thermogravimetry (TG) results, an intermediate sintering temperature of 400 °C corresponding to the removal of maximum amount of volatiles and decomposable materials was selected. Sintering temperatures above 800 °C proved to be ineffective probably due to the fibre/matrix interaction.

The infiltrated sol, in the inter-fibre region of the sample preforms, after gel formation followed by calcination may form agglomerates of particles at the intermediate sintering temperature of 400, 500 or 800 °C which undergoes densification after further sintering at higher temperatures, e.g. 1400 °C. Hence the strength of the CMCs has been found to depend to a great extent on its final sintering temperature which affects the degree of interaction between fibres and matrix. At a too high temperature, the material becomes brittle because of interfacial reaction, while at a too low temperature, the matrix does not sinter adequately [1,3]. This is supported by the strength values of the CMCs sintered at different temperatures (Table 2). Thus, an optimum sintering temperature is needed. It is to be noted that, in the present study, since the CMCs fabricated at the final sintering temperature of 1000 °C exhibited very low flexural strength, i.e. below 1 MPa, those values were not presented in Table 2.

3.3.3. In-situ deposition of carbon in CMCs

Intermediate heat treatment of the Sample nos. ZY5 and ZY6 of Table 2 at 500 °C for 1 h in air resulted in the formation of black coloured materials due to the in-situ deposition of carbon from the decomposable acetate groups present in the infiltrated preforms [17]. The black colour of the above materials is retained after final calcination at 1000 and 1400 °C in N_2 atmosphere. It is to be noted that the presence of carbon in the developed products corresponding to Sample nos. ZY5 and ZY6 of Table 2 caused an increase in their flexural strengths in comparison with that obtained for Sample no. ZY1 (free from carbon). Further, comparing the results of the Sample no. ZY1 (modulus value 3 GPa) and ZY5 (modulus value 51 GPa), it is observed that the presence of carbon in the fibre/matrix composite material significantly increased the modulus values and pseudo ductility in the materials. This may be explained to be due to the fact that the in situ deposition of carbon in the composite material presumably protected the fibre/matrix interface from strong interaction and acted as the crack arrester [18–20]. This is discernible from the load–displacement curve of the three-point bend test in Fig. 8 and the fibre pull-out from the SEM of Fig. 9 of

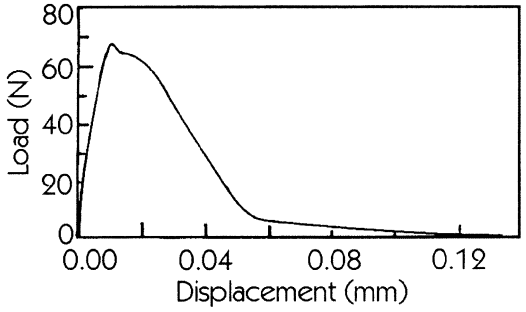

Fig. 8. Load–displacement curve of sample no. ZY6 of Table 2.

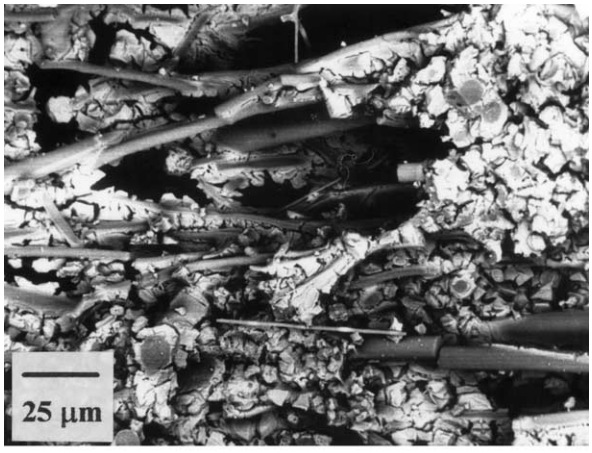

Fig. 9. SEM of the fracture surface of the carbon containing CMC after three-point bend test (sample no. ZY6 of Table 2).

Table 3
XRD results of CMCs calcined at different temperatures

Sol designation	Calcination temperature (°C)	Duration (h)	Crystalline phases
ZY	1000	1	c- + t-ZrO_2
	1200	1	c- + t-ZrO_2
	1400	1	c- + t-ZrO_2
A	1000	1	γ + δ-Al_2O_3
	1200	1	α-Al_2O_3
	1400	1	α-Al_2O_3
AS	1000	1	γ-Al_2O_3 + SiO_2 (amorphous)
	1200	1	Mullite (orthorhombic)
	1400	1	Mullite (orthorhombic)
AZ	1000	1	γ-Al_2O_3 + t-ZrO_2
	1200	1	α-Al_2O_3 + t-ZrO_2
	1400	1	α-Al_2O_3 + t-ZrO_2

Fig. 10. SEM of the fracture surface of the CMC (sample no. A2 of Table 2) showing multiple fracture of the matrix.

the same sample. Therefore, instead of using carbon-coated fibres as the reinforcement agents, the in situ deposited carbon in the bulk matrix may also modify the fibre/matrix interface and act as the crack arrester.

3.3.4. Crystallisation behaviour of the CMCs

CMCs fabricated after calcining at 1000, 1200 and 1400 °C, each with a dwell time of 1 h, were examined by XRD and the identified crystalline phases are presented in Table 3. It is to be noted that the phases other than mullite (fibre preform) crystallised at different temperatures from the matrix part of the CMCs have been listed in Table 3.

Considering the flexural strength values in Table 2 and XRD phases in Table 3, it is to be noted that the CMCs fabricated from the alumina sol exhibited the lowest flexural strength compared with those developed from the other three sols, irrespective of the final sintering temperature. The fracture surface of the Sample no. A2 of Table 2 as a typical case, under SEM showed the presence of considerable amounts of cracks in the matrix part of the matenals, as indicated in Fig. 10 The above phenomenon may be due to the reconstructive transformation of the transient phases, e.g. γ- and δ-Al_2O_3 to the stable phase α-Al_2O_3 during heat-treatment up to 1400 °C followed by grain growth with temperature, and thereby degrading the mechanical properties [21,22].

Addition of 13 mol% ZrO_2 to the Al_2O_3 matrix, however, exhibited an increase in the flexural strength at the same temperature. Crystallisation of t-ZrO_2 in the alumina matrix is believed to inhibit the growth of the α-Al_2O_3, resulting in the increase in strength values [23,24]. Similarly, incorporation of 40 mol% SiO_2 in the alumina matrix caused crystallisation of orthorhombic mullite at 1200–1400 °C and thereby helped to increase the flexural strength of the fabricated CMCs (Table 2) [25]. Further, XRD of the CMCs infiltrated with the ZY sol followed by sintering at the 1400 °C confirmed the presence of both c- and t- ZrO_2, along with the mullite

(preform), without any formation of monocliic polymorphs. Obviously, the Y_2O_3 additive in the matrix materials helped to retain t-ZrO_2 at 1400 °C by inhibiting grain growth [14], thus increasing the flexural strength of the CMCs and developing pseudo ductile character in the materials.

From the foregoing discussion, it may be stated that the flexural strength of the CMCs fabricated from the four different sols decreased in the order:

ZY > AS > AZ > A

Therefore, bonding at the fibre/matrix interface can be tailored by changing the characteristics of the infiltrate, number of infiltration, intermediate and final sintering temperatures, addition of non-reactive fillers, and finally via in situ deposition of carbon in the fibre/matrix composite materials by proper choice of carbon generating decomposable groups present in the corresponding precursor sols.

4. Conclusions

1. The sol–gel vacuum infiltration technique is very effective for the fabrication of near-net-shape CMCs using discontinuous mullite fibre preform having 15 vol.% of fibre content and various sols (in single- and bi-component oxide systems) as the infiltrate.
2. Effects of sol viscosity, number of infiltration, in situ deposition of carbon in the composite materials, characteristics of the infiltrates and calcination temperature on physicomechanical properties of CMCs are examined. Multiple infiltrations and presence of fillers in the infiltrates has been found to be effective for the development of CMCs with pseudo ductile characteristics.
3. The pseudo ductile character developed in the CMCs is evident from the load–elongation curve of the three-point bend test.
4. SEM indicates fibre pull-out in the fracture surface of the CMCs.

Acknowledgements

The authors thank Dr. H.S. Maiti, Director, Central Glass & Ceramic Research Institute (CG&CRI) and Dr. N. Ramakrishnan, Director, Regional Research Laboratory, Bhopal for their kind permission to publish this paper. The authors sincerely thank Dr. K.K. Phani, Head, Composite Division, for providing valuable suggestions throughout this work. They also thank colleagues of the X-ray, SEM, Composite, Refractories and Analytical Chemistry Sections for their kind help in materials characterization. Financial assistance provided by the Aeronautics Research and Development Board (AR&DB), Ministry of Defence, Govt. of India, is also thankfully acknowledged.

References

[1] R.S. Russel-Floyd, B. Harris, R.G. Cooke, J. Laurie, F.W. Hammett, R.W. Jones, et al., Application of sol–gel processing techniques for the manufacture of fibre-reinforced ceramics, J. Am. Ceram. Soc. 76 (10) (1993) 2635–2643.
[2] K.K. Chawla, Ceramic Matrix Composites, Chapman and Hall, UK, 1993.
[3] H.-K. Liu, W.-S. Kuo, B.-H. Lin, Pressure infiltration of sol–gel processed short fibre ceramic matrix composites, J. Mater. Sci. 33 (8) (1998) 2095–2101.
[4] J.R. Strife, J.J. Brennan, K.M. Prewo, Status of continuous fibre-reinforced ceramic matrix composite processing technology, Ceram. Eng. Sci. Proc. 11 (7–8) (1990) 871–919.
[5] J.A. Cornie, Y.-M. Chiang, D.R. Uhlmann, A. Mortensen, J.M. Collins, Processing of metal and ceramic matrix composites, Am. Ceram. Soc. Bull. 65 (2) (1986) 293–304.
[6] T.M. Besmann, J.C. Mclaughlin, R.A. Lowden, E. Lara-Curzio, Development of short fiber, SiC-based composites, in: J.P. Singh, N.P. Bansal, E. Ustundag (Eds.), Advances in Ceramic Matrix Composites VI, Am. Ceram. Soc, Westerville, OH, 2001, pp. 43–51.
[7] J. Brandt, K. Rundgren, R. Pompe, H. Swan, C. O'Meara, R. Lundberg, et al., SiC continuous fibre-reinforced Si_3N_4 by infiltration and reaction bonding, Ceram. Eng. Sci. Proc. 13 (9-10) (1992) 622–631.
[8] S.-M. Sim, R.I. Kerans, Slurry infiltration of 3-D woven composites, Ceram. Eng. Sci. Proc. 13 (9–10) (1992) 632–641.
[9] A. Dey, M. Chatterjee, M. K. Naskar, K. Basu, Near-net-shape fibre reinforced ceramic matrix composites by the sol infiltration technique, Mater. Lett. 57 (2003) 2919–2126.
[10] X. Gu, P.A. Trusty, E.G. Butler, C.B. Ponton, Deposition of zirconia sols on woven fibre preforms using a dip-coating technique, J. Eur. Ceram. Soc. 20 (6) (2000) 675–684.
[11] H.-K. Liu, B.-H. Lin, The effect of sol/particle reaction on properties of two-dimensional ceramic matrix composites, Mater. Lett. 48 (3–4) (2001) 230–241.
[12] E.H. Moore, 3-D composite fabrication through matrix slurry pressure infiltration, Ceram. Eng. Sci. Proc. 15 (4) (1994) 113–120.
[13] M. Chatteijee, D. Enkhtuvshin, B. Siladitya, D. Ganguli, Hollow alumina microspheres from boehmite sols, J. Mater. Sci. 33 (20) (1998) 4937–4942.
[14] P.K. Chakrabarty, M. Chatteijee, M.K. Naskar, B. Siladitya, D. Ganguli, Zirconia fibre mats prepared by a sol–gel spinning technique, J. Eur. Ceram. Soc. 21 (3) (2001) 355–361.
[15] M.K. Naskar, D. Ganguli, Rare-earth doped zirconia fibres by sol–gel processing, J. Mater. Sci. 31 (23) (1996) 6263–6267.
[16] A. Dey, M. Chatteijee, M.K. Naskar, S. Dalui, K. Basu, A novel technique for fabrication of near-net-shape CMCs, Bull. Mater. Sci. 25 (6) (2002) 493–495.
[17] M. Chatterjee, M.K. Naskar, D. Ganguli, Synthesis of polycrystalline ZrO_2–CaO fibres by sol–gel processing and their characterization, Trans. Ind. Ceram. Soc. 52 (2) (1993) 51–55.
[18] C.A. Doughan, R.L. Lehman, V.A. Greenhut, Interfacial properties of C-coated alumina fiber/glass matrix fiber composites, Ceram. Eng. Sci. Proc. 10 (7–8) (1989) 912–924.
[19] R.W. Rice, J.R. Spann, D. Lewis, W. Coblenz, The effect of ceramic fiber coatings on the room temperature mechanical behaviour of ceramic-fiber composites, Ceram. Eng. Sci. Proc. 5 (4) (1984) 614–624.

[20] K.A. Keller, T. Mah, T.A. Parthasarathy, C.M. Cooke, Fugitive interfacial carbon coatings for oxide/oxide composites, J. Am. Ceram. Soc. 83 (2) (2000) 329–336.
[21] C. Rastetter, W.R. Symes, Alumina fibre—a polycrystalline refractory fibre for use up to 1600 °C, Interceram 31 (3) (1982) 215–220.
[22] J.L. Mcardle, G.L. Messing, Transformation and microstructure controll in boehmite-derived alumina by ferric oxide seeding, Adv. Ceram. Mater. 3 (4) (1988) 387–392.
[23] C. Li, Y.W. Chen, T.-M. Yen, The effects of preparation method on the characteristics of alumina–zirconia powders, J. Sol–Gel Sci. Tech. 4 (3) (1995) 205–215.
[24] S. Bhaduri, S.B. Bhaduri, E. Zhou, Auto ignition synthesis and consolidation of Al_2O_3–ZrO_2 nano/nano composite powders, J. Mater. Res. 13 (1) (1998) 156–165.
[25] M. Chatteijee, M.K. Naskar, P.K. Chakrabarty, D. Ganguli, Sol–gel alumina fibre mats for high-temperature applications, Mater. Lett. 57 (1) (2002) 87–93.